

A generalized algebraic difference approach allows an improved estimation of aboveground biomass dynamics of *Cunninghamia lanceolata* and *Castanopsis sclerophylla* forests

Xiaolu Tang¹ · Lutz Fehrmann¹ · Fengying Guan² · David I. Forrester³ · Rubén Guisasola³ · César Pérez-Cruzado¹ · Torsten Vor⁴ · Yuanchang Lu⁵ · Juan Gabriel Álvarez-González⁶ · Christoph Kleinn¹

Received: 17 July 2016 / Accepted: 21 October 2016 / Published online: 15 February 2017
© INRA and Springer-Verlag France 2017

Abstract

• **Key message** A generalized algebraic difference approach (GADA) developed in this study improved the estimation of aboveground biomass dynamics of *Cunninghamia lanceolata* (Lamb.) Hook and *Castanopsis sclerophylla* (Lindl.) Schott forests. This could significantly improve the fieldwork efficiency for dynamic biomass estimation without repeated measurements.

• **Context** The estimation of biomass growth dynamics and stocks is a fundamental requirement for evaluating both the capability and potential of forest carbon sequestration. However, the biomass dynamics of *Cunninghamia lanceolata*

and *Castanopsis sclerophylla* using the generalized algebraic difference approach (GADA) model has not been made to date.

• **Aims** This study aimed to quantify aboveground biomass (AGB, including stem, branch and leaf biomass) dynamics and AGB increment in *C. lanceolata* and *C. sclerophylla* forests by combining a GADA for diameter prediction with allometric biomass models.

• **Methods** A total of 12 plots for a *C. lanceolata* plantation and 11 plots for a *C. sclerophylla* forest were selected randomly from a 100 m × 100 m systematic grid placed over the study area. GADA model was developed based on tree ring data for each stand.

• **Results** GADA models performed well for diameter prediction and successfully predicted AGB dynamics for both stands. The mean AGB of the *C. lanceolata* stand ranged from 69.4 ± 7.7 Mg ha⁻¹ in 2010 to 102.5 ± 11.4 Mg ha⁻¹ in 2013, compared to 136.9 ± 7.0 Mg ha⁻¹ in 2010 to 154.8 ± 8.0 Mg ha⁻¹ in 2013 for *C. sclerophylla*. The stem was the main component of AGB stocks and production. Significantly higher production efficiency (stem production/leaf area index) and AGB increment was observed for *C. lanceolata* compared to *C. sclerophylla*.

Handling Editor: Barry Alan Gardiner

Contribution of co-authors Xiaolu Tang and César Pérez-Cruzado convinced the design of this study; Xiaolu Tang wrote the manuscript; Fengying Guan, David I Forrester, Rubén Guisasola Lutz Fehrmann and Torsten Vor conducted the fieldwork and revised the manuscript; Juan Gabriel Álvarez-González revised the SAS code and manuscript; Yuanchang Lu and Christoph Kleinn revised the manuscript.

Electronic supplementary material The online version of this article (doi:10.1007/s13595-016-0603-0) contains supplementary material, which is available to authorized users.

✉ Xiaolu Tang
lxtt2010@163.com

¹ Chair of Forest Inventory and Remote Sensing, Georg-August-Universität Göttingen, Büsingenweg 5, 37077 Göttingen, Germany

² Key Laboratory of Bamboo and Rattan, International Centre for Bamboo and Rattan, No. 8, Futong Dongdajie, Wangjing, Chaoyang District, Beijing 100102, People's Republic of China

³ Chair of Silviculture, Faculty of Environment and Natural Resources, Freiburg University, Tennenbacherstr. 4, 79108 Freiburg, Germany

⁴ Department of Silviculture and Forest Ecology of the Temperate Zones, Georg-August-Universität Göttingen, Büsingenweg 1, 37077 Göttingen, Germany

⁵ Department of Forest Management and Statistics, Institute of Forest Resource Information Techniques, Chinese Academy of Forestry, Dongxiaofu 2, Xiangshan Road, Haidian, Beijing 100091, People's Republic of China

⁶ Departamento de Ingeniería Agroforestal, Universidad de Santiago de Compostela. Escuela Politécnica Superior, Campus Universitario, 27002 Lugo, Spain

• **Conclusion** Dynamic GADA models could overcome the limitations posed by within-stand competition and limited biometric data, can be applied to study AGB dynamics and AGB increment, and contribute to improving our understanding of net primary production and carbon sequestration dynamics in forest ecosystems.

Keywords Aboveground biomass · Tree ring analysis · Basal area · Leaf area index · Production efficiency

1 Introduction

Forest biomass plays an important role in the mitigation of climate change caused by rising atmospheric CO₂ concentrations because around 50% of tree biomass is carbon (Bonan 2008; IPCC 2007). The estimation of biomass growth dynamics and stocks has become a fundamental requirement for evaluating both the capability and potential of forest ecosystems to sequester carbon (Gower et al. 1997). It represents the net carbon input from the atmosphere to vegetation and it has received great attention during the past few decades (Fang et al. 2003). Due to the practical difficulties in belowground biomass estimation, there has been a focus on aboveground biomass (AGB), and its dynamics have become an important topic in estimating the effects of afforestation, deforestation and the role of improved forest management on the global carbon balance (Nunes et al. 2013; Zianis and Mencuccini 2005). AGB is calculated as the sum of stem, branch and leaf biomass, which can be calculated by allometric models using easily measured variables, such as tree diameter at breast height (*dbh*) and height (Albert et al. 2014; Cai et al. 2013). However, due to the diversity of climatic zones, site conditions and tree species, different allometric models generate great discrepancies in biomass estimates (Neumann et al. 2016). Therefore, localized- and species-specific allometric models are encouraged for biomass estimates. Besides the allometric models, biogeochemical-mechanistic approaches, such as BIOME BGC (Pietsch et al. 2005), CLM (Lawrence et al. 2011) and C-FIX (Veroustraete et al. 2002), are effective tools to estimate regional or even global biomass.

AGB increment represents a major part of net primary production (NPP) and is a key element required to understand ecosystem processes (Foster et al. 2014). It can be measured as the difference in AGB between two points in time (Foster et al. 2014). Repeated measurements of inventory plots are commonly used to estimate AGB increment or to calibrate forest growth models that can be used to predict AGB increment (Landsberg and Gower 1997; Nunes et al. 2013). However, repeated measurements require long-term planning and resources. As an alternative to long-term growth data from inventory plots and growth models, tree ring analysis by coring trees or felling a sample of trees in new inventory plots

offers a retrospective approach to study forest biomass dynamics as long as past mortality, thinning or other disturbances are known (Foster et al. 2014; Liu et al. 2012; Woolley et al. 2015). Tree rings could provide reliable data on historical growth rates (Brienen and Zuidema 2006). Tree age and the long-term growth rate reflected in the tree ring width could be directly applied to estimate the development of biomass using allometric models. Tree ring analysis has successfully been used to estimate stand level AGB dynamics and carbon sequestration trends (Liu et al. 2012; Mund et al. 2002). For instance, the annual increment of woody biomass estimated by coring individual trees ranged from 1.3 to 4.5 Mg ha⁻¹ year⁻¹ (equaling 0.65–2.25 Mg C ha⁻¹ year⁻¹) in the main European forest types (Babst et al. 2014). Although the stand biomass dynamics have been successfully estimated using tree ring analysis of the standard trees (representing the mean diameter and height) in our previous published results (Tang et al. 2015), that study did not address the biomass dynamics of each individual tree, which is necessary for studying the stand development and competition. Alternatively, age-related growth models based on tree ring data from a sample of trees could be used to improve the efficiency of AGB increment estimation. Although there are many studies on age-related diameter growth models using a generalized algebraic difference approach (GADA) in different forest types (Gea-Izquierdo et al. 2008; Palahí et al. 2008; Tang 2015; Tomé et al. 2006; Wu et al. 2001), these GADA models are mainly used to predict diameter growth based on repeated measurements, with few studies focusing on AGB and AGB increment (Ogawa 2012). To our knowledge, there are so far no studies about predicting AGB increment using GADA models derived from tree ring analysis and individual-tree allometric biomass equations in *Cunninghamia lanceolata* (Lamb.) Hook and *Castanopsis sclerophylla* (Lindl.) Schott forests.

C. lanceolata is one of the most popular plantation tree species in subtropical China with relatively high timber quality and fast growth (Zhao et al. 2009). In the past few decades, the area of *C. lanceolata* has increased rapidly. According to the seventh national forest inventory of China, it covers an area of 8.54 million ha, which corresponds to 21% of the total plantation area in China (Jia et al. 2009). *C. lanceolata* plantations are usually managed in a clear cutting system with a relatively short rotation period of 25 years. Information about AGB increment with a sufficient accuracy over the rotation period is increasingly important to evaluate the carbon sequestration potential in the *C. lanceolata* forests and carbon market (Zhang et al. 2004), as well as the supply of biomass for bioenergy, timber industry and bio-based products.

C. sclerophylla is another important evergreen and shade-tolerant tree species. It is widely distributed across subtropical areas of China from 200 to 1000 m above sea level, and it is one of the dominant and native species in evergreen

broadleaved forests (An et al. 2001). *C. sclerophylla* plays a significant role in water and soil conservation (Li et al. 2011). It is also an economically important species because its seeds are used to produce tofu, which is a staple in the diet of many local residents. However, during the establishment of the *C. lanceolata* plantations for climate mitigation and timber production, many *C. sclerophylla* forests have been cleared.

The objectives of this study were to (1) develop GADA models to predict diameter at breast height (*dbh*, 1.3 m) at any age for each individual trees in *C. lanceolata* and *C. sclerophylla* forests; (2) estimate AGB dynamics and inter-annual variability in AGB increment using GADA models and allometric biomass models; (3) compare the production efficiency of the two species. The results will provide a better understanding of AGB dynamics of these two important species in subtropical China and the application of GADA models in AGB dynamic estimation.

2 Materials and methods

2.1 Study area

The study was conducted in the Jitan township of Shitai county (29°59′–30°24′ N, 117°12′–117°59′ E), in the Southern part of Anhui province, China (Fig. 1). It is a mountainous area with a forest cover of about 80%, an elevation range of 50 to 1000 m with an average elevation of 260 m. The soils mainly originated from limestones, moorstones and mudstones (Forest Bureau of Shitai County 2004). The region has a mid-subtropical, humid, mountainous climate with distinct seasonality (Geng and Wang 2011). The recorded annual average temperature is 16 °C but can vary from –13.2 to 40.9 °C (Lu 2010). The mean precipitation is 1668 mm with high inter-annual variability, with about 70% of annual precipitation occurring from April to September (Geng and Wang 2011). The average annual sunshine duration is 1704 h and evaporative capacity is 1256 mm (Lu 2010).

2.2 Plot design

One pure *Cunninghamia lanceolata* stand and one pure *Castanopsis sclerophylla* stand were selected for our study. Both stands had similar stand origins, originating from clear cuts of secondary forests. The area was 22 ha for *C. lanceolata* and 10 ha for *C. sclerophylla*. In the first 3 years after planting *C. lanceolata*, understory and grass were removed manually to improve the survival rate of seedlings. Poorly formed, dead and dying trees were removed from both stands in 2004. A thinning from below with an intensity of 10% (volume removal), or 13% (trees per ha removal), was conducted in the two stands in 2010 (unpublished document from local Forest Bureau). In each stand, a systematic base grid of

100 m × 100 m was established, from which six locations were chosen randomly to establish permanent plots while an additional temporary plot was installed 25 m north of each permanent plot for destructive biomass sampling. Altogether, 12 plots were installed for *C. lanceolata* and 11 plots for *C. sclerophylla*. A forest inventory was conducted from March to May 2013, during which, *dbh* of all trees, height of one dominant, co-dominant and suppressed tree, tree horizontal distance, azimuth, plot slope, elevation and coordinates were measured and recorded. Tree dominance was determined based on the *dbh*, height and crown layer distributions. The crown of dominant trees extends above the general layer of the stand and intercepts direct sunlight across the top and upper branches. The diameter is usually amongst the largest in the stand. The crown of co-dominant trees lies within the main layer. Tree diameter lies in the middle range in the stand. The crown of suppressed trees lies entirely below the main canopy. Tree diameter is amongst the smallest in the stand (Tang et al. 2015). The plot design was a nested circular plot with different horizontal radii for different tree diameter classes (Tang 2015). An inner smaller plot with a 6-m radius was used to include trees with a *dbh* between 10 and 20 cm, while trees with *dbh* larger than 20 cm were measured up to a horizontal distance of 10 m (Tang et al. 2015).

2.3 Biomass analysis

All trees in sample plots were numbered and assigned to three dominance classes—dominant, co-dominant and suppressed trees. A sample tree representing the average *dbh* and height in each dominance class was destructively sampled for AGB (including stems, branches and leaves), leaf area determination and stem analysis in the temporary plots. In total, 18 *C. lanceolata* and 15 *C. sclerophylla* trees were felled, which corresponded to six and five trees for each dominance class for *C. lanceolata* and *C. sclerophylla*, respectively. The *dbh* and tree height of sample trees of *C. lanceolata* ranged from 8.2 to 27.3 cm and 8.7 to 16.6 m, respectively, and were 12.9 to 28.4 cm and 8.1 to 15.9 m for the *dbh* and height of *C. sclerophylla*. Before felling, the *dbh* was measured to the nearest 0.1 cm with a diameter tape and the North direction was marked. After the trees were felled, the total tree height and the heights and diameters of all branches were measured.

Live branches (and additional dead branches, if applicable) from each tree were sampled to develop allometric equations for predicting branch and leaf biomass from branch diameter, and hence total tree branch biomass and leaf biomass. From the sampled branches, a subsample of leaves was randomly selected to determine the specific leaf area (SLA), which is the ratio of leaf area and leaf biomass (Guisasola 2014). For *C. sclerophylla*, a random selection of approximately 20 leaves per branch was used to obtain SLA. Due to the very high number of small leaves of *C. lanceolata*, a subsample per

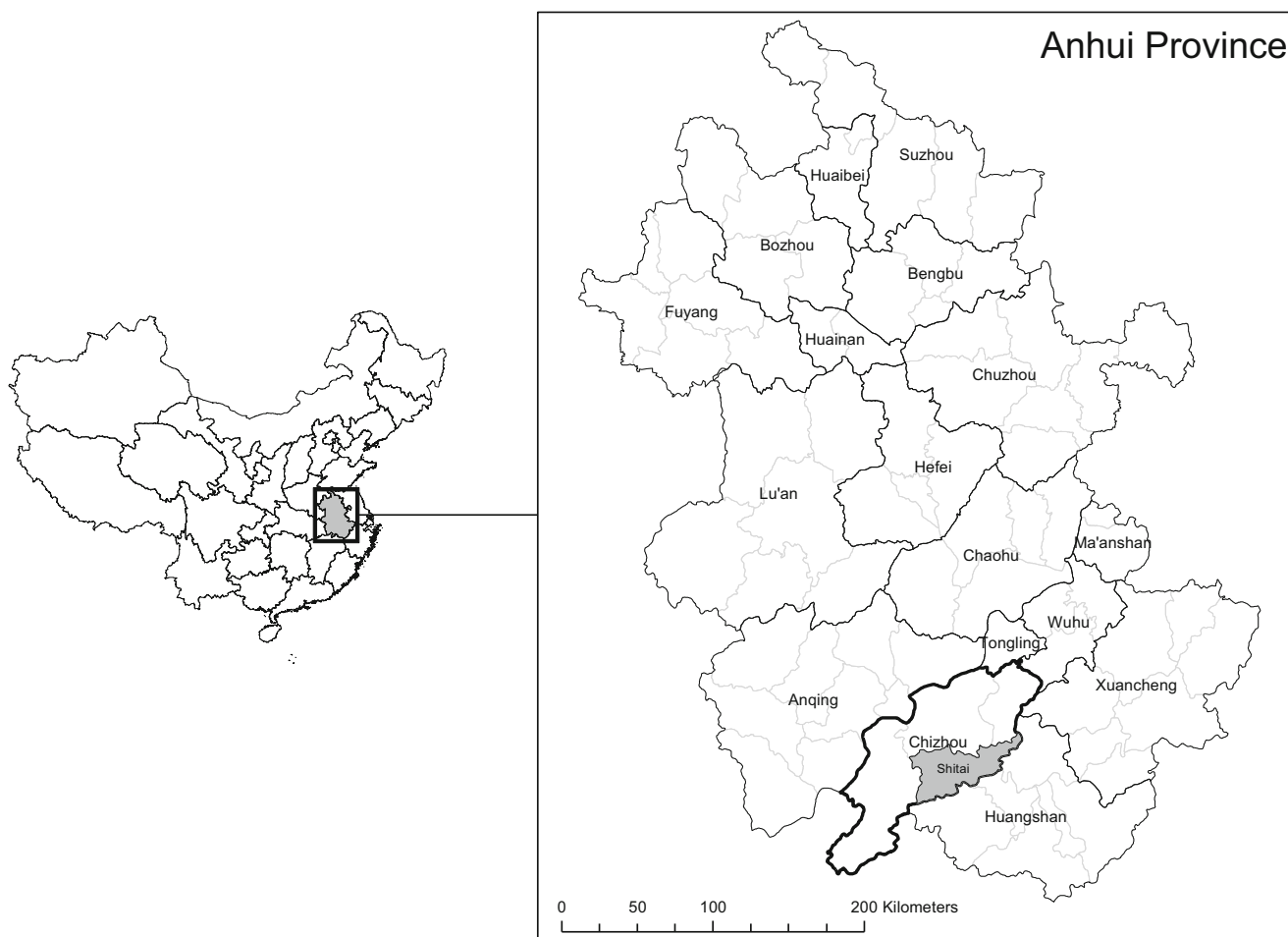


Fig. 1 Location of Shitai County in the southern part of Anhui Province, South-East China

branch was selected for SLA determination, as described in detail in Guisasola (2014). Leaves were scanned on an A3 scanner (Epson Expression 1000XL). The leaf area of each branch was calculated by multiplying its leaf mass with the SLA for that branch. Allometric branch mass and leaf area equations were then developed (Guisasola 2014) and used to predict the mass and leaf area of all branches, which was then summed up to the tree and the stand levels.

2.4 Stem analysis

Stems were cut into different sections at heights of 0.3, 1.3, 3 and 2-m intervals thereafter up to the treetop. Cross-sectional stem discs (about 5 cm thick) were cut at each of these heights, as well as one disc at ground level. If there was a branch at the height of the disc, a replacement disc was collected 5 cm above or below. In the end, 213 *C. lanceolata* discs and 119 *C. sclerophylla* discs were collected. To fit the GADA model for *dbh* predictions, 1 disc at breast height (1.3 m) of each felled tree was used, resulting in 18 *C. lanceolata* discs and 15 *C. sclerophylla* discs.

All branches, leaves and discs were dried at 100 °C to constant weight. The mean fresh to oven-dried weight ratios of the discs of a given tree were used to convert the whole stem fresh weight into dry biomass. The biomass of each individual tree was the sum of all biomass compartments. After drying, the discs were processed according to standard techniques applied in dendrochronology: the discs were sanded with progressively finer grades of sandpaper (up to 240 grits) to improve the visibility of year rings (Stokes 1996). The polished discs were rewetted and scanned at 1200 dpi resolution (Epson Expression 1000XL) and visually cross-dated by Lignovision and TSAPwin (LINTAB, RINNTECH, Inc. Freiburg) software. All the discs were cross-dated by matching wide and narrow rings to assign the same calendar year in four directions (East, West, North, and South) (Tang 2015). The annual diameter increments of each tree were calculated by averaging the cardinal radii and multiplying this value by two. The bark thickness was also measured. The tree diameter calculated from cross-dating was not equal to that measured in the field using a diameter tape due to the irregular growth rate of boles in different directions. Therefore diameters needed to be calibrated according to the

procedures proposed by Liu et al. (2012). Finally, annual diameter with bark was estimated according to following the processes (Bush and Brand 2008):

$$BR = \frac{B_T}{D_{OB}} = \frac{B_T}{(B_T + D_{IB})} \tag{1}$$

$$D_{OB} = \frac{D_{IB}}{1-BR} \tag{2}$$

Where BR is the bark ratio, B_T is the measured bark thickness from tree ring analysis, and D_{IB} and D_{OB} are the diameter inside and outside bark. The D_{OB} was calculated by dividing D_{IB} by 1-BR. This conversion was required because we developed the allometric models using D_{OB} as the input variable.

2.5 Development of GADA models

The GADA model was developed based on the model of Bertalanffy (1957), whose integral form can be expressed as follows:

$$Y = a_1(1-\exp(-a_2 \cdot t))^{a_3} \tag{3}$$

Where Y is the target variable; a_1 is an asymptote or limiting value; a_2 is a rate parameter, and a_3 is an initial pattern parameter; t is the tree age (years). To derive a model with both polymorphism and asymptote from Eq. 3, more than one parameter has to be site-specific (Álvarez-González et al. 2010; Cieszewski and Bailey 2000). Therefore, the asymptote parameter a_1 and the shape parameter a_3 are assumed to be dependent on the site, and a site parameter (X) was included into the model (in Eq. 4). To achieve such a derivation, the base equation is re-parameterized into a form that is more suitable for the manipulation of these two parameters (using $\exp(a'_1)$ instead of a_1 , and taking the natural logarithm of the function) as follows (Álvarez-González et al. 2010):

$$Y = \exp(a'_1)(1-\exp(-a_2 \cdot t))^{a_3} \tag{4}$$

$$\ln Y = a'_1 + a_3 \ln(1-\exp(-a_2 \cdot t)) \tag{5}$$

These site-dependent parameters are conditioned to be consistently proportional to each other's inverse over the site productivity by the following definitions:

$$a'_1 = X \text{ and } a_3 = b_2 + \frac{b_3}{X}, \text{ while } a_2 = b_1$$

Eq. 3 can be expressed as follows:

$$\ln Y = X + b_2 + \frac{b_3}{X} \ln(1-\exp(-b_1 \cdot t)) \tag{6}$$

The solution of X involves solving roots of a quadratic equation and a selection of the suitable root to substitute into

the dynamic equation. The selection process may depend on the equation parameters that in return depend on the data and the domain of the applicable ages (Cieszewski and Bailey 2000). With the initial condition value Y_0 and t_0 , the solution of Eq. 6 is expressed as follows:

$$X_0 = \frac{1}{2} \left((\ln Y_0 - b_2 L_0) \pm \sqrt{(\ln Y_0 - b_2 L_0)^2 - 4b_3 L_0} \right) \tag{7}$$

where $L_0 = \ln(1 - \exp(-b_1 t_0))$.

In this study, t_0 is the tree age in the year 2013 derived from the stem analysis, while Y_0 is the dbh in the year 2013.

According to the tree growth characteristics, the root most likely to be real and positive is selected. Thus, after substituting it into Eq. 6, the GADA formulation applied in our study is as follows:

$$Y = Y_0 \left[\frac{1 - \exp(-b_1 t)}{1 - \exp(-b_1 t_0)} \right]^{b_2 + \frac{b_3}{X_0}} \tag{8}$$

Although this model has commonly been applied to calculate site index (Alvarez-González et al. 2010; Sharma et al. 2011) and basal area (Alvarez-González et al. 2010; Barrianta et al. 2006), some authors have successfully applied this model for diameter prediction (Gea-Izquierdo et al. 2008). GADA formulations using different base models such as the log-logistic or the Hossfeld models can also be analysed (Cieszewski 2002); however, the GADA model (Eq. 8) was used because comparing the performance of different GADA models is not the focus of this study and Eq. 8 could achieve our objectives.

2.6 Model fitting

All the possible growth intervals were used to fit the GADA model; therefore, autocorrelated residuals are expected because the database contains multiple observations for each individual tree. This, however, violates the assumption of independent error terms. Therefore, we corrected the autocorrelation using a modified continuous autoregressive error structure (mCAR(x)). To account for first-order autocorrelation, a mCAR(1) model form can be used which expands the error terms according to Eq. 9 (Álvarez-González et al. 2010):

$$e_{ij} = d_i \rho_1^{h_{ij} - h_{ij-1}} e_{ij-1} + \varepsilon_{ij} \tag{9}$$

where e_{ij} is the j th ordinary residual on the i th individual (i.e. the difference between the observed and the estimated diameters of the tree i at height measurement j), $d_i = 1$ for $j > 1$ and it is zero for $j = 1$, ρ_1 is the first-order continuous autoregressive parameter to be estimated, and $h_{ij} - h_{ij-1}$ is the distance separating the j th from the j th-1 observations within each tree, $h_{ij} > h_{ij-1}$. ε_{ij} is an independent normal random variable with a mean value of zero. To test for the presence

Table 1 Structural characteristics of *C. lanceolata* and *C. sclerophylla* stands in 2013 (mean \pm standard error)

Stands	Age at bottom discs (years)	Mean <i>dbh</i> (cm)	Mean <i>H</i> (m)	<i>N</i> (stems ha ⁻¹)	BA (m ² ha ⁻¹)	LAI (m ² m ⁻²)	Volume (m ³ ha ⁻¹)	Mean biomass (Mg ha ⁻¹ year ⁻¹)
<i>C. lanceolata</i>	17	16.2 \pm 0.3a	11.6 \pm 0.1a	1553 \pm 200b	33.4 \pm 3.8a	5.4 \pm 0.6a	200.1 \pm 22.7a	6.0 \pm 0.7b
<i>C. sclerophylla</i>	52	19.0 \pm 0.4a	11.4 \pm 0.2a	990 \pm 77a	30.1 \pm 1.5a	6.9 \pm 0.4b	202.3 \pm 10.2b	3.0 \pm 0.0a

dbh is diameter at breast height (1.3 m); *H* is the mean height of all trees; *N* is the number of trees per hectare; BA is the stand basal area; LAI is the leaf area index. Different letters in the same column indicate significant differences ($p < 0.05$, ANOVA). Volume of *C. lanceolata* is calculated from the compatible taper function (Tang et al. 2016), while volume of *C. sclerophylla* is calculated by the allometric models derived from the felled trees

of autocorrelation, we used the Durbin-Watson test. The modified mCAR(1) error structure was programmed in the MODEL procedure of SAS/ETS® (SAS Institute Inc 2007), which allows for dynamic updating of the residuals.

Heteroscedasticity could lead to non-minimum variance parameter estimates and unreliable predictor intervals. To avoid this problem, the error variance was assumed to be a power function of the predicted diameter (Huang et al. 2000). The weighting factor (W_i) was:

$$W_i = \frac{1}{\text{Pred}.dt_i^k} \quad (10)$$

where k is a constant; $\text{Pred}.dt_i$ is the predicted values from the fitted model. Generally, $k = -2, -3/2, -1, -1/2, 1/2, 1, 3/2, 2$. Since the predicted diameters are initially unknown, weighting is an iterative process. In our study, $k = 3/2$ showed the best results based on plots of studentized residuals against the predicted diameter.

2.7 Estimation of AGB and AGB increment

Allometric models are widely used to estimate tree biomass, either for the biomass of different biomass compartments or the tree as a whole (González-García et al. 2013; Xiang et al. 2011). The tree-level allometric models for each biomass compartment are given in Supplement Table S1. The stem, branch and leaf biomass and leaf area of all trees was calculated in the inventory plots and scaled to the reference area of 1 ha by considering an expansion factor (32 for 10-m radius plots and 88 for 6-m radius plots) for the year 2013. The total AGB of 2013 was calculated as the sum of stem, branch and leaf biomass. Following the same procedure, biomass compartment, total AGB and leaf area of 2012, 2011 and 2010 were calculated using these allometric models and the diameter of each individual tree estimated using Eq. 8. Consequently, AGB increment was calculated as the sum of the biomass increment of stems, branches and leaves of each tree per inventory plot. AGB increment of plants with *dbh* < 10 cm was ignored because it is assumed to contribute less than 5% to the total AGB increment for these forests and is difficult to measure in the field (Yang et al. 2010). Since a

thinning from below took place in 2010 without precise data acquisition (extracted volume, tree heights and *dbh*), we only estimated AGB and AGB increment for the period from 2010 to 2013. We also assumed that there was no mortality after the thinning in 2010, which is consistent with the absence of any dead trees in both stands.

2.8 Data analysis

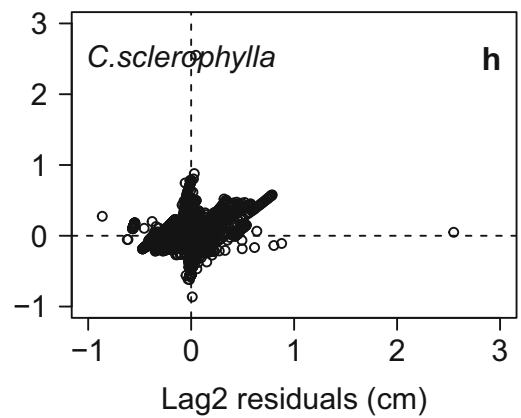
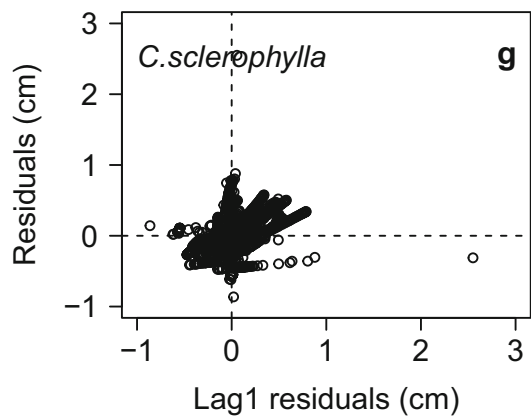
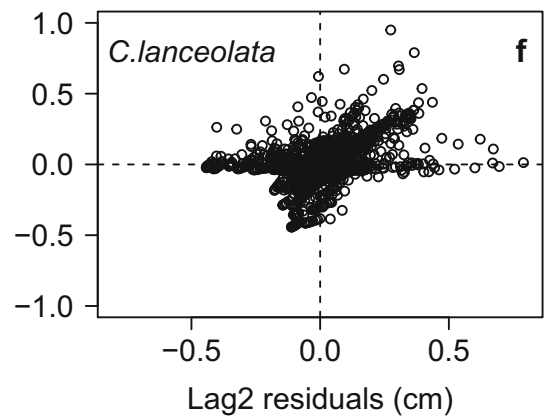
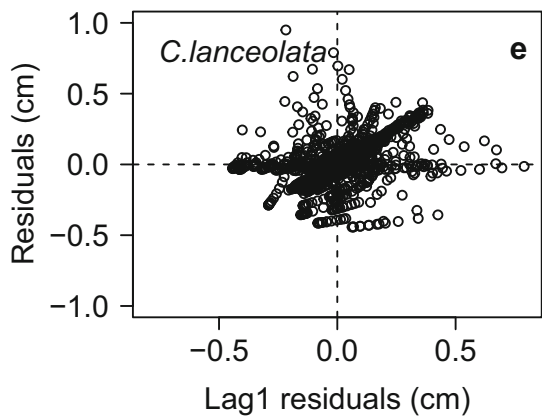
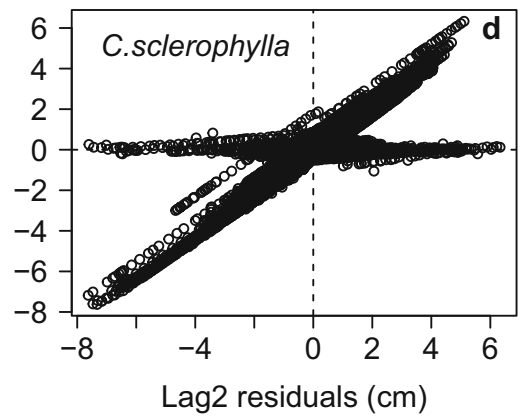
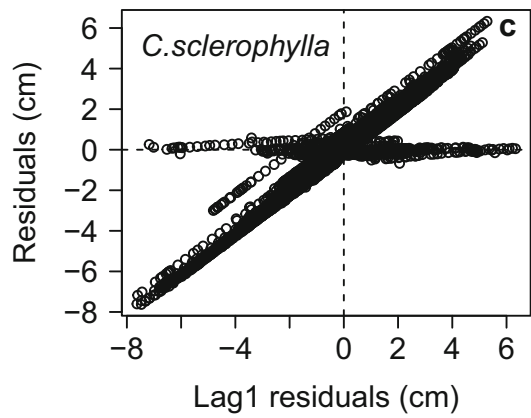
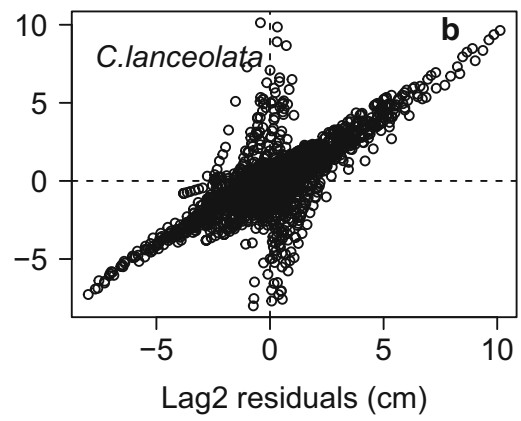
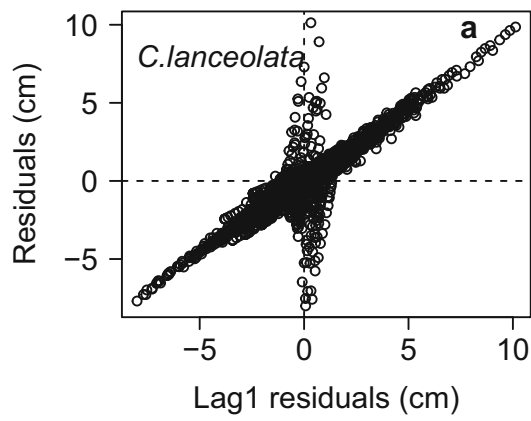
Linear regression was applied to examine the relationships between stand basal area and AGB or AGB increment. One-way ANOVA was used to test for significant differences in stand characteristics, biomass compartment, production efficiency (stem biomass production/leaf area index), AGB and AGB increment. Statistical analyses were performed using R (R Core Team 2014).

3 Results

3.1 Stand characteristics

The stand characteristics of the two studied stands are shown in Table 1. Although there was a large difference in age between *C. lanceolata* and *C. sclerophylla* stands, no significant difference was found for mean stand height, basal area or stand volume (all $p > 0.05$). However, leaf area index (LAI) of the *C. lanceolata* stand was $5.4 \pm 0.6 \text{ m}^2 \text{ m}^{-2}$, (mean \pm standard error) which was significantly lower than that of the *C. sclerophylla* stand (6.9 ± 0.4 ; $p = 0.049$). Mean stand biomass followed the reverse trend such that the *C. lanceolata* stand was two times of that in the *C. sclerophylla* stand.

Fig. 2 Residuals against lag1 and lag2 residuals for the GADA model before (a)–(d) and after (e)–(h) using a first-order continuous time autoregressive error structure for *C. lanceolata* and *C. sclerophylla* forests ($n = 4534$ for *C. lanceolata* and $n = 30,142$ for *C. sclerophylla*). Lag1 and lag 2 mean one lag residual and two lag residuals from previous observations of tree diameter, respectively



3.2 Performance of the GADA model

At first, the models were fitted without considering any autocorrelation. There was a strong linear trend in the residuals as a function of lag1 residuals (one lag residual from previous observations of tree diameter) for both stands (Fig. 2a–d). This indicated a strong autocorrelation among the multiple observations in each tree. Therefore, a first-order continuous time autoregressive error structure was derived. By considering this autocorrelation, although the trend in residuals as a function of lag1 residuals did not disappear completely, the trend was clearly reduced (Fig. 2e–h). The only purpose of eliminating autocorrelation was to improve the statistical interpretation of the model, and it has no practical use unless repeated measurements were conducted in the sample plot (Álvarez-González et al. 2010; Diéguez-Aranda et al. 2006). All parameter estimates were significant at the 0.001 level (Table 2). The GADA model performed very well when predicting tree diameters for both stands. We observed an adjusted R^2 of 0.94 for the *C. lanceolata* stand and an adjusted R^2 of 0.96 for the *C. sclerophylla* stand, with a RMSE of 1.810 and 1.308 cm for both stands, respectively.

3.3 AGB and AGB increment

The total AGB of *C. lanceolata* was 69.4 ± 7.7 Mg ha⁻¹ in 2010, increasing to 80.0 ± 8.9 , 91.0 ± 10.1 and 102.5 ± 11.4 Mg ha⁻¹ in 2011, 2012 and 2013, respectively (Table 3). These values were significantly lower than those of the *C. sclerophylla* stand ($p < 0.05$). Stem biomass contributed 75%–76% to the total AGB for both stands. Branch and leaf biomass contributed 14% and 11%, respectively, to the total AGB for the *C. lanceolata* stand, compared to 21% and 3%, respectively, for the *C. sclerophylla* stand. Although the stem and branch biomass of the *C. lanceolata* stand was significantly lower than that of the *C. sclerophylla* stand, the leaf biomass

of *C. lanceolata* was about twice as high as that of *C. sclerophylla*. Total AGB was strongly correlated with stand basal area for both stands (Fig. 3).

AGB increment showed a reverse trend of the AGB such that AGB increment of *C. lanceolata* was significantly higher ($p < 0.05$) than that of *C. sclerophylla* for the three-year period (Fig. 4). AGB increment of *C. lanceolata* was 10.6 ± 1.2 for 2010–2011, 11.0 ± 1.2 for 2011–2012 and 11.5 ± 1.3 Mg ha⁻¹ year⁻¹ for 2012–2013, respectively, compared to 5.8 ± 0.3 , 5.9 ± 0.3 and 6.3 ± 0.4 Mg ha⁻¹ year⁻¹ for the *C. sclerophylla* stand. Stem biomass increment was the main contributor to AGB increment. As expected, leaf biomass increment contributed least to AGB increment with a value of 8% for *C. lanceolata* and 1.5% for *C. sclerophylla*. There was no significant inter-annual variability in compartment-wise biomass increment and total AGB increment for the two stands. Again, strong relationships between AGB increment and stand basal area were found with values of the adjusted R^2 of 0.96 for *C. lanceolata* and 0.69 for *C. sclerophylla* (Fig. 5).

To further compare the AGB increment of the two stands, AGB increment at the age of 16 years was estimated (Fig. 6) using the GADA model and the allometric biomass equations. AGB increments of stem, branch and leaf of *C. lanceolata* at age 16 years were significantly higher than those of *C. sclerophylla* ($p < 0.01$). Total AGB increment was 11.5 ± 1.3 Mg ha⁻¹ year⁻¹ for *C. lanceolata* and 1.5 ± 0.1 Mg ha⁻¹ year⁻¹ for *C. sclerophylla*.

The production efficiency was defined as the ratio of stem production and leaf area index because the carbon sequestration in stem biomass is much larger than that of other compartments (Nunes et al. 2013). As expected, stem production efficiency of *C. lanceolata*, ranging from 1.8 to 2.0, was significantly higher than that of the *C. sclerophylla* stand for the 3 years observed ($p < 0.001$) (about 0.8, Fig. 7), indicating that *C. lanceolata* is a fast-growing and efficient species. This can

Table 2 Estimated regression coefficients and goodness-of-fit statistics of Eq. 8

Stand	Coefficient	Estimate	SE	<i>p</i> value	Number ^a	RMSE (cm)	Adjusted R^2
<i>C. lanceolata</i>	b_1	0.0575	0.00340	<0.001	4534	1.810	0.935
	b_2	0.858	0.0300	<0.001			
	b_3	0.441	0.0888	<0.001			
	ρ_1	1.581	0.0626	<0.001			
<i>C. sclerophylla</i>	b_1	0.0153	0.000212	<0.001	30,142	1.308	0.956
	b_2	0.261	0.0244	<0.001			
	b_3	2.805	0.0879	<0.001			
	ρ_1	1.670	0.00661	<0.001			

ρ_1 is the autoregressive parameter; SE is the standard error of the estimate; RMSE is the root mean square error and adjusted R^2 is the adjusted coefficient of determination

^a All the possible growth intervals were used; therefore, the sample size was expanded to 4534 for *C. lanceolata* and 30,142 for *C. sclerophylla*

Table 3 Stem, branch, leaf and total AGB (Mg ha^{-1}) of the *C. lanceolata* and *C. sclerophylla* stands from 2010 to 2013, Mean \pm standard error (percentage of total AGB in each biomass compartment, $n = 12$ for *C. lanceolata* and $n = 11$ for *C. sclerophylla*)

Stands	Stem	Branch	Leaf	Total AGB
Biomass 2013				
<i>C. lanceolata</i>	$78.0 \pm 8.7(76.1\%)a$	$14.1 \pm 1.5(13.8\%)a$	$10.4 \pm 1.2(10.1\%)b$	$102.5 \pm 11.4a$
<i>C. sclerophylla</i>	$118.5 \pm 6.4(76.5\%)b$	$31.83 \pm 1.5(20.6\%)b$	$4.5 \pm 0.2(2.9\%)a$	$154.8 \pm 8.0b$
Biomass 2012				
<i>C. lanceolata</i>	$68.6 \pm 7.7(75.4\%)a$	$12.8 \pm 1.4(14.0\%)a$	$9.6 \pm 1.1(10.5\%)b$	$91.0 \pm 10.1a$
<i>C. sclerophylla</i>	$113.3 \pm 6.0(76.3\%)b$	$30.8 \pm 1.5(20.7\%)b$	$4.4 \pm 0.2(2.9\%)a$	$148.5 \pm 7.6b$
Biomass 2011				
<i>C. lanceolata</i>	$60.1 \pm 6.7(75.1\%)a$	$11.3 \pm 1.2(14.1\%)a$	$8.7 \pm 1.0(10.7\%)b$	$80.0 \pm 8.9a$
<i>C. sclerophylla</i>	$108.5 \pm 5.8(76.1\%)b$	$29.8 \pm 1.5(20.9\%)b$	$4.3 \pm 0.2(3.0\%)a$	$142.6 \pm 7.3b$
Biomass 2010				
<i>C. lanceolata</i>	$51.9 \pm 5.8(74.8\%)a$	$10.8 \pm 1.0(14.1\%)a$	$7.7 \pm 0.9(11.0\%)b$	$69.4 \pm 7.7a$
<i>C. sclerophylla</i>	$103.9 \pm 5.5(75.9\%)b$	$28.7 \pm 1.5(21.0\%)b$	$4.2 \pm 0.2(3.1\%)a$	$136.9 \pm 7.0b$

Different letters in the same column indicate significant differences ($p < 0.05$)

be confirmed by the mean stand biomass (Table 1) and AGB increment (Fig. 4).

4 Discussion

4.1 Development of GADA model

In our study, GADA models were developed based on data from tree ring analyses to predict *dbh* at any age for each individual tree. The GADA models were flexible enough to predict diameter increment at any time intervals, such as two- or five-year intervals, which allowed us to reconstruct historical diameters. Using tree-individual allometric biomass

models to estimate tree compartment biomass combined with the GADA model, AGB dynamics and annual AGB increment were successfully estimated from 2010 to 2013. Such estimates of AGB increment are urgently needed to reduce uncertainties in ecosystem production and associated feedback to climate change (Frank et al. 2010). The dynamic GADA models could overcome the limitations of within-stand competition and limited biometric data and improve our understanding of net primary production in these forest ecosystems. In addition, the methodology described in the present paper is that the *dbh* and biomass increments can be assessed much quicker than with a permanent experiment where *dbh* is re-measured in several points in time. This methodology may be of interest for developing growth models in remote areas (or in other conditions) where the establishment of permanent plots is unaffordable. Another advantage of our approach is that the complete *dbh* growth pattern with age is reconstructed, something which may be unaffordable with permanent plots which are being re-measured regularly. The final advantage of our method is that the growing conditions of a given stand can be modelled quickly. The lag between the growing conditions and obtaining the data in permanent plots is so large that this is not a suitable method for developing models for the actual climatic conditions. To develop GADA models, there are two basic approaches used to gain the tree ring data: collecting increment cores (Babst et al. 2014; Foster et al. 2014; Groenendijk et al. 2014) or collecting complete discs after felling the trees (Brienen and Zuidema 2006; Groenendijk et al. 2014; Mbow et al. 2013). Collecting the increment cores is quicker and less destructive than sampling complete discs. However, caution is needed with tree ring analyses from increment cores because the difficulty in separating true year rings and false rings can lead to a significant bias. This is especially important for *C. lanceolata* where false rings are frequent and there is a high probability of incorrectly

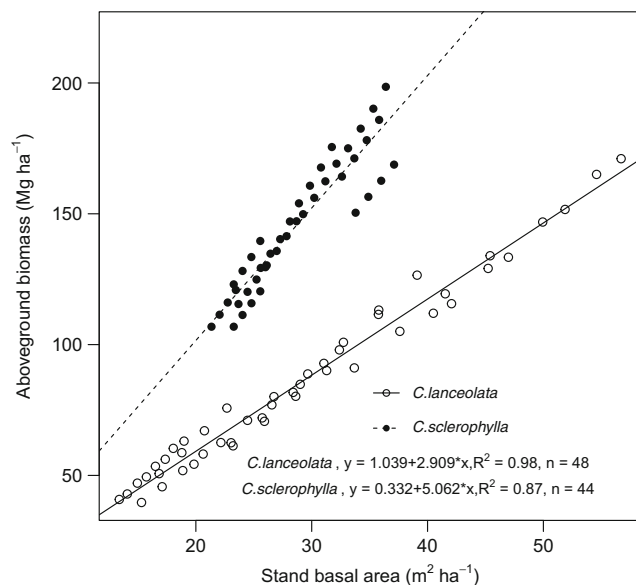
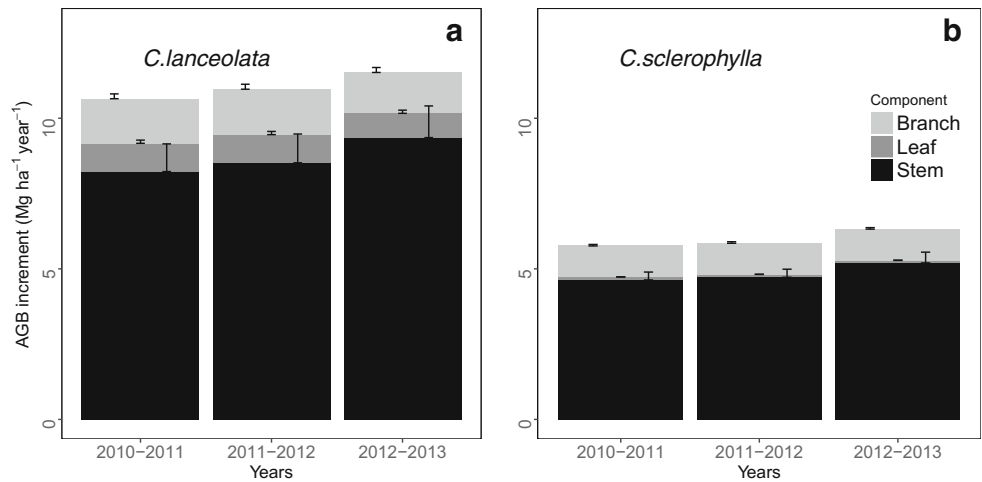


Fig. 3 Relationships between aboveground biomass and stand basal area for *C. lanceolata* and *C. sclerophylla* forests. For both linear regressions, a significance level of $p < 0.001$ was achieved

Fig. 4 Inter-annual biomass increment of stem, branch and leaf from 2011 to 2013 for *C. lanceolata* (a) and *C. sclerophylla* (b) forests ($n = 12$ for *C. lanceolata* and $n = 11$ for *C. sclerophylla*). The error bars mean the standard error



classifying false rings when using increment cores. Another problem that arises from increment cores is associated with no-pith cores, because stems are not always round when growing on a slope, due to competition and other stressors, even though there are many approaches to predict the missing rings (Brienen and Zuidema 2006; Groenendijk et al. 2014). Therefore, as for many other species (Liu et al. 2012; Maingi 2006), complete discs are preferred.

However, because the quality of the fit does not necessarily reflect the quality of the prediction, assessment of their validity is often needed to ensure that the predictions represent the most likely outcome in the real world (Yang et al. 2004). The only method that can be regarded as “true” validation involves the use of a new independent data set (Pretzsch et al. 2002; Yang et al. 2004), but the scarcity of such data forces the use of alternative approaches. The common method of splitting the data set in two portions does not provide additional information (Huang et al. 2003), and according to Myers (1990) and Hirsch (1991), the final estimation of the model parameters

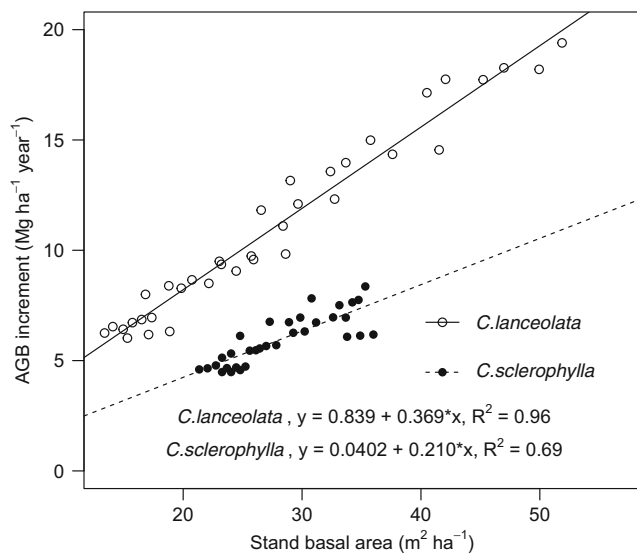


Fig. 5 Relationships between AGB increment stand basal area

should come from the entire data set, because the estimates obtained with this approach will be more precise than those obtained with the model fitted from only one portion of the data. Moreover, other techniques such as double cross-validation or statistical testing provide very limited information about the predictive ability of the models (Kozak and Kozak 2003; Yang et al. 2004). Therefore, we decided to defer model validation until a new data set is available for assessing the quality of the predictions.

4.2 Leaf area index

LAI is strongly related to carbon uptake, transpiration, leaf respiration, light variability and stand growth and structure (Chen et al. 1997; Moser et al. 2007; Olivas et al. 2013), and therefore affects many biological and physical processes in

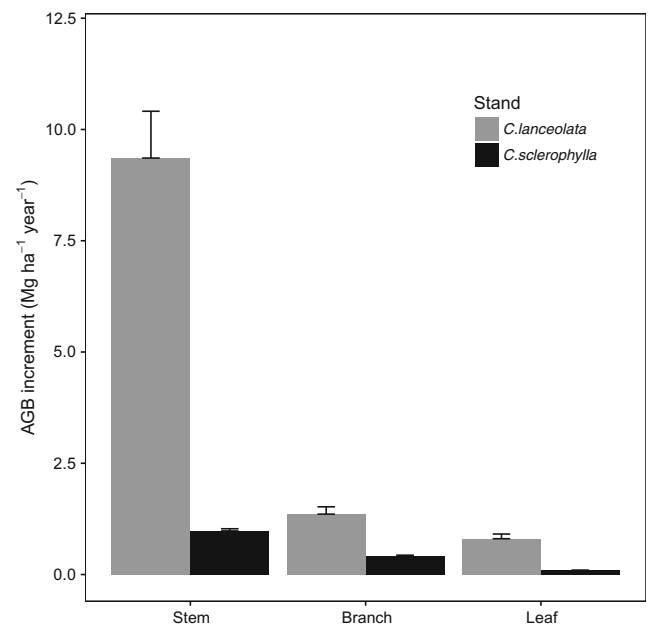


Fig. 6 Comparison of AGB increment at age of 16 years for *C. lanceolata* and *C. sclerophylla* forests

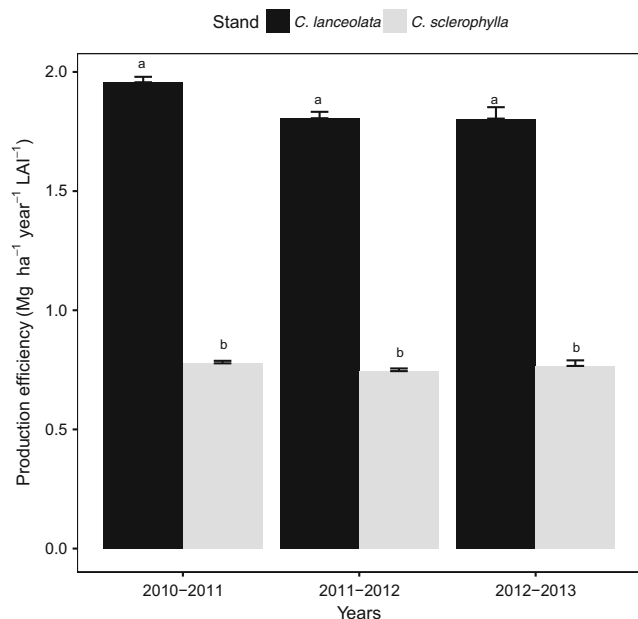


Fig. 7 Production efficiency (stem production/leaf area index) for *C. lanceolata* and *C. sclerophylla* forests. Different letters above the error bars indicate significant differences between the tree species ($p < 0.05$) ($n = 12$ for *C. lanceolata* and $n = 11$ for *C. sclerophylla*). The error bars mean the standard error

plant canopies (Chen et al. 1997). The average LAI in 2013 was $5.4 \pm 0.6 \text{ m}^2 \text{ m}^{-2}$ for the *C. lanceolata* stand, which is close to the world average leaf area index ($5.55 \pm 4.14 \text{ m}^2 \text{ m}^{-2}$) based on a meta-analysis of 809 field plots in a literature review by Luo et al. (2002). Other authors have reported lower leaf area indices for this species, for example, $4.3 \text{ m}^2 \text{ m}^{-2}$ in Qianyanzhou, subtropical China (Li et al. 2007). The leaf area index of the *C. sclerophylla* stand ($6.9 \text{ m}^2 \text{ m}^{-2}$) was significantly higher than for the *C. lanceolata* stand ($p = 0.049$). This is consistent with Luo et al. (2002) who report that the LAI in China is commonly $>6 \text{ m}^2 \text{ m}^{-2}$ for tropical rainforest, subtropical evergreen broadleaved forest and temperate mixed forest.

4.3 Comparisons of AGB

As expected, AGB increased with age for both stands, which agrees with other studies (Chen et al. 2013; Chen 1998). The AGB of *C. sclerophylla* was significantly higher than that of *C. lanceolata*. Similar results were found for *Castanopsis kawakamii* forests that had a significantly higher AGB compared to nearby *C. lanceolata* forests (Yang et al. 2006). This was mainly due to the differences in wood density of the two species. Although the stand volume was similar (Table 1), the wood density was 0.40 kg m^{-3} for *C. lanceolata* and 0.64 kg m^{-3} for *C. sclerophylla* according to our measured data. Difference in ages was another important reason for the differences in AGB. It is generally recognized that AGB increases with stand age for young forests (Chen et al. 2013;

Foster et al. 2014). In our study, the *C. lanceolata* stand was 17 years old, while the *C. sclerophylla* stand was 52 years old (Table 1).

AGB of the *C. lanceolata* stand was $102.5 \pm 11.4 \text{ Mg ha}^{-1}$ in 2013 (Table 3), which was comparable to a *C. lanceolata* stand with similar stand age in Huitong, Hunan Province (106 Mg ha^{-1}) (Xiao et al. 2007). But it was higher than inventory-based national average biomass (80 Mg ha^{-1}) of *C. lanceolata* (Guo et al. 2010) and a *C. lanceolata* stand in Guangxi Province (86 Mg ha^{-1}) (Bing et al. 2009). Other authors observed higher values with an average of 155 Mg ha^{-1} in a 17-year *C. lanceolata* stand in Tongdao County (Chen 1998) and 160 Mg ha^{-1} in Nanping City (Chen et al. 2013). Similarly, AGB of *C. sclerophylla* was $154.8 \pm 8.0 \text{ Mg ha}^{-1}$ in 2013, which lies in the range of reported biomass of the main forest types in China ($48.8\text{--}215.8 \text{ Mg ha}^{-1}$) (Guo et al. 2010). It is higher than that of natural *Castanopsis carlesii*–*Schima superba* mixed stands in the Xiaokeng region of the Nanling Mountains, in subtropical China (115.2 Mg ha^{-1}) (Xie et al. 2013) but lower than the mean AGB in *Castanopsis*, *Cinnamomum* and *Schima superba* forests in China (256.4 Mg ha^{-1}) (Jiang et al. 1999). These differences in AGB are mainly related to inherent variations in growth rates, stand age, stand density and starting *dbh* (Houghton 2005; Jandl et al. 2007; Pan et al. 2004). For example, the AGB of *C. lanceolata* with a stand age of 40 years was twice as high as a 21-year-old stand (Chen et al. 2013). However, even with a similar age, site and climate conditions, the AGB of *C. lanceolata* in our study was lower than that reported by Chen et al. (2013) due to the high stand density of the latter study ($2800\text{--}3875 \text{ trees ha}^{-1}$ versus $1553 \text{ trees ha}^{-1}$ in our study), indicating how stand density can be used to increase stand biomass (Jandl et al. 2007).

Stem mass was the dominant AGB compartment for every stand and contributed 76% to total AGB on average. This is consistent with *C. lanceolata* forests in Taiwan (80%, Yen and Lee 2011), the Huitong national research station of forest ecosystems (78%, Wang et al. 2013) and the northwest Fujian Province in subtropical China (72%, Huang et al. 2013). This value is also very similar to the mean ratio of stem biomass to AGB in forest ecosystems across China (79%, Cheng et al. 2007).

4.4 Annual AGB increment

AGB increment of the *C. lanceolata* stand was 10.6 ± 1.2 for 2010–2011, 11.0 ± 1.2 for 2011–2012 and $11.5 \pm 1.3 \text{ Mg ha}^{-1} \text{ year}^{-1}$ for 2012–2013. These values were significantly higher than those of the *C. sclerophylla* stand (Fig. 5). This can be explained by the tree physiology, structural characteristics of individual trees and the stand age (McMurtrie et al. 1994; Nunes et al. 2013). The young age in *C. lanceolata* could potentially lead to a higher AGB increment because it

is generally accepted that the biomass accumulation reaches its maximum relatively early in the life of a stand, and thereafter declines with forest age (Acker et al. 2002; Ryan et al. 1997).

Because there were large age difference between the two stands (17 years and 52 years), the comparison of AGB increment at the same age was more meaningful. For simplicity, AGB increment at age 16 years was estimated and AGB increment of *C. lanceolata* was significantly higher than that of *C. sclerophylla* (Fig. 6). The results indicated that the carbon sequestration rate of *C. lanceolata* was significantly higher than that of *C. sclerophylla*. It should be noted that the AGB increment of the trees thinned in 2010, and tree mortality during stand development for both stands was not included because such data was not available in this study, as mentioned above. However, thinning from below and tree mortality often occur more among small trees in these stands (Zhang et al. 2015); therefore, it is believed that these trees only account for a small part of the total AGB increment and their exclusion will not have significantly influenced the predicted AGB increment trend. Moreover, these results should be considered with caution due to the large simulation period used to estimate the AGB increment of *C. sclerophylla* (36 years). By considering only the *dbh* increment, a constant height/*dbh* relationship is assumed, an assumption which is reasonable for the specific conditions of this study, as all the field plots were established in a relatively homogeneous area.

In this study, the AGB increment of *C. lanceolata* was higher than the average net primary production of main forest types in China ($3.5\text{--}6.7\text{ Mg ha}^{-1}\text{ year}^{-1}$) (Fang et al. 2003). The AGB increment of the *C. sclerophylla* stand ranged from $5.8 \pm 0.3\text{ Mg ha}^{-1}\text{ year}^{-1}$ for 2010–2011 to $6.3 \pm 0.4\text{ Mg ha}^{-1}\text{ year}^{-1}$ for 2010–2011. It was comparable to the AGB increment of spruce, secondary birch and secondary conifer-broadleaved forests (about $6\text{ Mg ha}^{-1}\text{ year}^{-1}$) at ages from 30 to 50 years in Sichuan province, subtropical China (Zhang et al. 2012), and higher than the mixed *Schima superba*–*Castanopsis carlesii* forests in subtropical China ($3.9\text{ Mg ha}^{-1}\text{ year}^{-1}$) (Yang et al. 2010). However, the value was lower than the national average AGB increment of the evergreen broadleaved forests in China (Fang et al. 2003).

5 Conclusions

Understanding biomass dynamics is a fundamental requirement for evaluating the carbon sequestration capabilities and potentials of forest ecosystems. In this study, AGB dynamics and AGB increment from 2010 to 2013 of *C. lanceolata* and *C. sclerophylla* were successfully estimated by using GADA models and allometric biomass models. The stand AGB of *C. sclerophylla* was significantly higher than that of *C. lanceolata*, and stem contributed 76% to the total AGB in

both stand types, highlighting the importance of the stem production in carbon sequestration of forest ecosystems.

The high determination coefficients of the GADA models for both stands indicated that GADA models are a powerful tool to predict the diameter dynamics. Although repeated measurements are most accurate for increment estimation, GADA model developed using tree ring data were far more efficient and easy to operate. These dynamic models can overcome the limitations of within-stand competition and limited biometric data and can be applied to study biomass dynamics. If mortality data are available, the GADA models could contribute to the prediction of long-term biomass dynamics without repeated measurements in the field and improve our understanding of the net primary production in forest ecosystems.

Acknowledgements Xiaolu Tang conducted this research as a part of his dissertation at Georg-August-Universität Göttingen (Tang 2015). This study was part of Sino-German Cooperation on Innovative Technologies and Service Capacities of Multifunctional Forest Management (Lin²Value 033L049-CAFYBB2012013) funded by the Federal Ministry of Education and Research (BMBF) and the Chinese Academy of Forestry, “Twelfth Five-year” National Technology Support Program (2012BAD23B04). We thank Hans Fuchs, Sabine Schreiner, Haijun Yang and Dengkui Mo from the Georg-August-Universität Göttingen for plot design and fieldwork support. We also thank Director An’guo Fan, Mr. Bailing Ding, Miss Yue’e Chu from the Shitai Forest bureau for kindly organizing the fieldwork. Lastly, special thanks to Mr. Xiaozhu Wang and Mr. Hongbing Ruan for fieldwork support.

Compliance with ethical standards

Funding This study was part of Sino-German Cooperation on Innovative Technologies and Service Capacities of Multifunctional Forest Management (Lin²Value 033L049-CAFYBB2012013) funded by the Federal Ministry of Education and Research (BMBF) and the Chinese Academy of Forestry, “948 project” of State Forest Administration (No. 2013-4-70), special research fund of International Centre for Bamboo and Rattan (No. 1632013010) supported by International Centre for Bamboo and Rattan (ICBR) in China.

References

- Acker SA, Halpern CB, Harmon ME, Dyrness CT (2002) Trends in bole biomass accumulation, net primary production and tree mortality in *Pseudotsuga menziesii* forests of contrasting age. *Tree Physiol* 22: 213–217. doi:10.1093/treephys/22.2.3.213
- Albert K, Annighöfer P, Schumacher J, Ammer C (2014) Biomass equations for seven different tree species growing in coppice-with-standards forests in Central Germany. *Scand J For Res* 29:1–12. doi:10.1080/02827581.2014.910267
- Álvarez-González JG, Zingg A, Klaus Von G (2010) Estimating growth in beech forests: a study based on long term experiments in Switzerland. *Ann For Sci* 67:307–307. doi:10.1051/forest/2009113
- An S, Liu M, Wang Y, Li J, Chen X, Li G, Chen X (2001) Forest plant communities of the Baohua Mountains, eastern China. *J Veg Sci* 12: 653–658. doi:10.2307/3236905
- Babst F, Bouriaud O, Alexander R, Trouet V, Frank D (2014) Toward consistent measurements of carbon accumulation: a multi-site

- assessment of biomass and basal area increment across Europe. *Dendrochronologia* 32:153–161. doi:10.1016/j.dendro.2014.01.002
- Barrio-Anta M, Castedo-Dorado F, Diéguez-Aranda U, Álvarez-González JG, Parresol BR, Rodríguez-Soalleiro R (2006) Development of a basal area growth system for maritime pine in northwestern Spain using the generalized algebraic difference approach. *Can J For Res* 36:1461–1474. doi:10.1139/x06-028
- Bertalanffy VL (1957) Quantitative laws in metabolism and growth. *Q Rev Biol* 32:217–231
- Bing K, ShiRong L, DaoXiong C, LiHua L (2009) Characteristics of biomass, carbon accumulation and its spatial distribution in *Cunninghamia lanceolata* forest ecosystem in low subtropical area. *Sci Silvae Sin* 45:147–153 (in Chinese with English abstract)
- Bonan GB (2008) Forests and climate change: forcings, feedbacks, and the climate benefits of forests. *Science* 320:1444–1449. doi:10.1126/science.1155121
- Brienen RJW, Zuidema PA (2006) The use of tree rings in tropical forest management: projecting timber yields of four Bolivian tree species. *For Ecol Manag* 226:256–267. doi:10.1016/j.foreco.2006.01.038
- Bush R, Brand G (2008) Lake states (LS) variant overview: forest vegetation simulator. USDA Forest Service, Forest Management Service Center. Fort Collins, CO
- Cai S, Kang X, Zhang L (2013) Allometric models for aboveground biomass of ten tree species in northeast China. *Ann for Res* 56: 105–122
- Chen H (1998) Biomass and nutrient distribution in a Chinese-fir plantation chronosequence in Southwest Hunan, China. *For Ecol Manag* 105:209–216. doi:10.1016/S0378-1127(97)00284-3
- Chen JM, Rich PM, Gower ST, Norman JM, Plummer S (1997) Leaf area index of boreal forests: theory, techniques, and measurements. *J Geophys Res Atmos* 102:29429–29443. doi:10.1029/97jd01107
- Chen GS, Yang ZJ, Gao R, Xie JS, Guo JF, Huang ZQ, Yang YS (2013) Carbon storage in a chronosequence of Chinese fir plantations in southern China. *For Ecol Manag* 300:68–76. doi:10.1016/j.foreco.2012.07.046
- Cheng DL, Wang GX, Li T, Tang QL, Gong CM (2007) Relationships among the stem, aboveground and total biomass across Chinese forests. *J Integr Plant Biol* 49:1573–1579. doi:10.1111/j.1774-7909.2007.00576.x
- Cieszewski CJ (2002) Comparing fixed- and variable-base-age site equations having single versus multiple asymptotes. *For Sci* 48:7–23
- Cieszewski C, Bailey RL (2000) Generalized algebraic difference approach: theory based derivation of dynamic site equations with polymorphism and variable asymptotes. *For Sci* 46:116–126
- Diéguez-Aranda U, Castedo-Dorado F, Álvarez-González JG, Rojo A (2006) Compatible taper function for Scots pine plantations in northwestern Spain. *Can J For Res* 36:1190–1205. doi:10.1139/x06-008
- Fang J et al (2003) Increasing net primary production in China from 1982 to 1999. *Front Ecol Environ* 1:293–297. doi:10.1890/1540-9295(2003)001[0294:INPPIC]2.0.CO;2
- Forest Bureau of Shitai County (2004) Forest resources planning and design survey of Shitai County in 2004. Hefei, China
- Foster JR, D'Amato AW, Bradford JB (2014) Looking for age-related growth decline in natural forests: unexpected biomass patterns from tree rings and simulated mortality. *Oecologia* 175:363–374. doi:10.1007/s00442-014-2881-2
- Frank DC, Esper J, Raible CC, Buntgen U, Trouet V, Stocker B, Joos F (2010) Ensemble reconstruction constraints on the global carbon cycle sensitivity to climate. *Nature* 463:527–530. doi:10.1038/nature08769
- Gea-Izquierdo G, Cañellas I, Montero G (2008) Site index in agroforestry systems: age-dependent and age-independent dynamic diameter growth models for *Quercus ilex* in Iberian open oak woodlands. *Can J For Res* 38:101–113. doi:10.1139/x07-142
- Geng TS, Wang HH (2011) Research on the water and soil conservation in Shitai County of Anhui Province. *J Anhui Agri Sci* 39(451–452): 482 (in Chinese with English abstract)
- González-García M, Hevia A, Majada J, Barrio-Anta M (2013) Above-ground biomass estimation at tree and stand level for short rotation plantations of *Eucalyptus nitens* (Deane & Maiden) Maiden in Northwest Spain. *Biomass Bioenergy* 54:147–157. doi:10.1016/j.biombioe.2013.03.019
- Gower ST, Vogel JG, Norman JM, Kucharik CJ, Steele SJ, Stow TK (1997) Carbon distribution and aboveground net primary production in aspen, jack pine, and black spruce stands in Saskatchewan and Manitoba, Canada. *J Geophys Res Atmos* 102:29029–29041. doi:10.1029/97jd02317
- Groenendijk P, Sass-Klaassen U, Bongers F, Zuidema PA (2014) Potential of tree-ring analysis in a wet tropical forest: a case study on 22 commercial tree species in Central Africa. *For Ecol Manag* 323:65–78. doi:10.1016/j.foreco.2014.03.037
- Guisasola R (2014) Allometric biomass equations and crown architecture in mixed-species forests of subtropical China. Master thesis, Albert-Ludwigs Universität Freiburg
- Guo ZD, Fang JY, Pan YD, Birdsey R (2010) Inventory-based estimates of forest biomass carbon stocks in China: a comparison of three methods. *For Ecol Manag* 259:1225–1231. doi:10.1016/j.foreco.2009.09.047
- Hirsch RP (1991) Validation samples. *Biometrics* 47:1193–1194
- Houghton RA (2005) Aboveground forest biomass and the global carbon balance. *Glob Chang Biol* 11:945–958. doi:10.1111/j.1365-2486.2005.00955.x
- Huang S, Price D, Titus S (2000) Development of ecoregion-based height-diameter models for white spruce in boreal forests. *For Ecol Manag* 129:125–141. doi:10.1016/S0378-1127(99)00151-6
- Huang S, Yang Y, Wang Y (2003) A critical look at procedures for validating growth and yield models. In: A Amaro, D Reed, P Soares (eds) Modelling forest systems. CAB International, Wallingford, pp 271–293
- Huang ZQ, He ZM, Wan XH, Hu ZH, Fan SH, Yang YS (2013) Harvest residue management effects on tree growth and ecosystem carbon in a Chinese fir plantation in subtropical China. *Plant Soil* 364:303–314. doi:10.1007/s11104-012-1341-1
- IPCC (2007) Climate Change 2007: synthesis report. Contribution of Working Groups I, II and III to the Fourth Assessment Report of the Intergovernmental Panel on Climate Change. Intergovernmental Panel on Climate Change. Geneva
- Jandl R et al (2007) How strongly can forest management influence soil carbon sequestration? *Geoderma* 137:253–268. doi:10.1016/j.geoderma.2006.09.003
- Jia Z, Zhang J, Wang X, Xu J, Li Z (2009) Report for Chinese forest resource—the 7th national forest inventory. China Forestry Publishing House, Beijing (in Chinese)
- Jiang H, Apps MJ, Zhang Y, Peng C, Woodard PM (1999) Modelling the spatial pattern of net primary productivity in Chinese forests. *Ecol Model* 122:275–288. doi:10.1016/S0304-3800(99)00142-8
- Kozak A, Kozak R (2003) Does cross validation provide additional information in the evaluation of regression models? *Can J For Res* 33: 976–987. doi:10.1139/x03-022
- Landsberg JJ, Gower ST (1997) Applications of physiological ecology to forest management. Academic Press, San Diego
- Lawrence D, Oleson K, Flanner M (2011) Parameterization improvements and functional and structural advances in version 4 of the community land model. *Journal of Advanced Model Earth System* 3:M03001
- Li X, Liu Q, Cai Z, Ma Z (2007) Specific leaf area and leaf area index of conifer plantations in Qianyanzhou station of subtropical China. *J Plant Ecol* 31:93–101 (in Chinese with English abstract)
- Li K, Jang H, You M, Zeng B (2011) Effect of simulated nitrogen deposition on soil respiration of *Lithocarpus glaber* and *Castanopsis*

- sclerophylla*. Acta Ecol Sin 31:82–89 (in Chinese with English abstract)
- Liu YC, Zhang YD, Liu SR (2012) Aboveground carbon stock evaluation with different restoration approaches using tree ring chronosequences in Southwest China. For Ecol Manag 263:39–46. doi:10.1016/j.foreco.2011.09.008
- Lu CM (2010) Rock-soil geochemical features for Dashan Area, Shitai, Anhui. Geolo Anhui 20:120–125 (in Chinese with English abstract)
- Luo T, Neilson RP, Tian H, Vörösmarty CJ, Zhu H, Liu S (2002) A model for seasonality and distribution of leaf area index of forests and its application to China. J Veg Sci 13:817–830. doi:10.1111/j.1654-1103.2002.tb02111.x
- Mainigi JK (2006) Growth rings in tree species from the Tana river floodplain, Kenya. J East Afr Nat Hist 95:181–211. doi:10.2982/0012-8317(2006)95[181:GRITSF]2.0.CO;2
- Mbow C, Chhin S, Sambou B, Skole D (2013) Potential of dendrochronology to assess annual rates of biomass productivity in savanna trees of West Africa. Dendrochronologia 31:41–51. doi:10.1016/j.dendro.2012.06.001
- McMurtrie RE, Gholz HL, Linder S, Gower ST (1994) Climatic factors controlling the productivity of pine stands: a model-based analysis. Ecol Bull 43:173–188
- Moser G, Hertel D, Leuschner C (2007) Altitudinal change in LAI and stand leaf biomass in tropical montane forests: a transect study in Ecuador and a pan-tropical meta-analysis. Ecosystems 10:924–935. doi:10.1007/s10021-007-9063-6
- Mund M, Kummert E, Hein M, Bauer GA, Schulze ED (2002) Growth and carbon stocks of a spruce forest chronosequence in central Europe. For Ecol Manag 171:275–296. doi:10.1016/S0378-1127(01)00788-5
- Myers RH (1990) Classical and modern regression with applications, vol 2, 2nd edn. Duxbury, Belmont
- Neumann M et al (2016) Comparison of carbon estimation methods for European forests. For Ecol Manag 361:397–420. doi:10.1016/j.foreco.2015.11.016
- Nunes L, Lopes D, Rego FC, Gower ST (2013) Aboveground biomass and net primary production of pine, oak and mixed pine-oak forests on the Vila Real district, Portugal. For Ecol Manag 305:38–47. doi:10.1016/j.foreco.2013.05.034
- Ogawa K (2012) Mathematical analysis of age-related changes in leaf biomass in forest stands. Can J For Res 42:356–363. doi:10.1139/X11-192
- Olivas PC, Oberbauer SF, Clark DB, Clark DA, Ryan MG, O'Brien JJ, Ordoñez H (2013) Comparison of direct and indirect methods for assessing leaf area index across a tropical rain forest landscape. Agric For Meteorol 177:110–116. doi:10.1016/j.agrformet.2013.04.010
- Palahi M, Pukkala T, Kasimiadis D, Poirazidis K, Papageorgiou AC (2008) Modelling site quality and individual-tree growth in pure and mixed *Pinus brutia* stands in north-east Greece. Ann For Sci 65:501–501. doi:10.1051/forest:2008022
- Pan YD, Luo TX, Birdsey R, Hom J, Melillo J (2004) New estimates of carbon storage and sequestration in China's forests: effects of age-class and method on inventory-based carbon estimation. Clim Chang 67:211–236. doi:10.1007/s10584-004-2799-5
- Pietsch SA, Hasenauer H, Thornton PE (2005) BGC-model parameters for tree species growing in central European forests. For Ecol Manag 211:264–295. doi:10.1016/j.foreco.2005.02.046
- Pretzsch H et al (2002) Recommendations for standardized documentation and further development of forest growth simulators. Forstwissenschaftliches Centralblatt 121:138–151
- R Core Team (2014) R: a language and environment for statistical computing. R Foundation for Statistical Computing, Vienna URL <http://www.R-project.org/>. Accessed 6 Mar 2015
- Ryan MG, Binkley D, Fownes JH (1997) Age-related decline in forest productivity: pattern and process. In: Begon M, Fitter AH (eds) Advances in ecological research, vol 27. Academic Press, Cambridge, pp 213–262
- SAS Institute Inc (2007) SAS user's guide, version 9.2. SAS Institute Cary, Cary
- Sharma RP, Brunner A, Eid T, Øyen BH (2011) Modelling dominant height growth from national forest inventory individual tree data with short time series and large age errors. For Ecol Manag 262: 2162–2175. doi:10.1016/j.foreco.2011.07.037
- Stokes MA (1996) An introduction to tree-ring dating. University of Arizona Press, Tucson
- Tang X (2015) Estimation of biomass, volume and growth of subtropical forests in Shitai County, China. Dissertation, Georg-August-University Göttingen
- Tang X, Lu Y, Fehrmann L, Forrester DI, Guisasa-Rodríguez R, Pérez-Cruzado C, Kleinn C (2015) Estimation of stand-level aboveground biomass dynamics using tree ring analysis in a Chinese fir plantation in Shitai County, Anhui Province, China. New Forest 47:319–332. doi:10.1007/s11056-015-9518-0
- Tomé J, Tomé M, Barreiro S, Paulo JA (2006) Age-independent difference equations for modelling tree and stand growth. Can J For Res 36:1621–1630. doi:10.1139/x06-065
- Veroustraete F, Sabbe H, Eerens H (2002) Estimation of carbon mass fluxes over Europe using the C-Fix model and Euroflux data. Remote Sens Environ 83:376–399. doi:10.1016/S0034-4257(02)00043-3
- Wang QK, Wang SL, Zhong MC (2013) Ecosystem carbon storage and soil organic carbon stability in pure and mixed stands of *Cunninghamia lanceolata* and *Michelia macclurei*. Plant Soil 370: 295–304. doi:10.1007/s11104-013-1631-2
- Woolley TJ, Harmon ME, O'Connell KB (2015) Inter-annual variability and spatial coherence of net primary productivity across a western Oregon Cascades landscape. For Ecol Manag 335:60–70. doi:10.1016/j.foreco.2014.09.028
- Wu C, Hong W, Jiang Z (2001) Simulation of *Cunninghamia lanceolata* growth by wave-type time series analysis. J App Eco 12:659–662 (in Chinese with English abstract)
- Xiang W et al (2011) General allometric equations and biomass allocation of *Pinus massoniana* trees on a regional scale in southern China. Ecol Res 26:697–711. doi:10.1007/s11284-011-0829-0
- Xiao FM, Fan SH, Wang SL, Xiong CY, Zhang C, Liu SP, Zhang J (2007) Carbon storage and spatial distribution in *Phyllostachy pubescens* and *Cunninghamia lanceolata* plantation ecosystem. Acta Ecol Sin 27:2794–2801 (in Chinese with English abstract)
- Xie TT, Li G, Zhou GY, Wu ZM, Zhao HB, Qiu ZJ, Liang RY (2013) Aboveground biomass of natural *Castanopsis carlesii-Schima superba* community in Xiaokeng of Nanling Mountains, South China. J App Eco 24:2399–2407 (in Chinese with English abstract)
- Yang Y, Monserud RA, Huang S (2004) An evaluation of diagnostic tests and their roles in validating forest biometric models. Can J For Res 34:619–629. doi:10.1139/X03-230
- Yang Y, Chen G, Wang Y, Xie J, Yang S, Zhong X (2006) Carbon storage and allocation in *Castanopsis kawakamii* and *Cunninghamia lanceolata* plantations in subtropical China. Sci Silvae Sin 42:43–47 (in Chinese with English abstract)
- Yang T, Song K, Da L, Li X, Wu J (2010) The biomass and aboveground net primary productivity of *Schima superba-Castanopsis carlesii* forests in east China. Sci China Life Sci 53:811–821. doi:10.1007/s11427-010-4021-5
- Yen T, Lee J (2011) Comparing aboveground carbon sequestration between moso bamboo (*Phyllostachys heterocycla*) and China fir (*Cunninghamia lanceolata*) forests based on the allometric model. For Ecol Manag 261:995–1002. doi:10.1016/j.foreco.2010.12.015
- Zhang XQ, Kirschbaum MUF, Hou ZH, Guo ZH (2004) Carbon stock changes in successive rotations of Chinese fir (*Cunninghamia lanceolata* (Lamb) Hook) plantations. For Ecol Manag 202:131–147. doi:10.1016/j.foreco.2004.07.032

- Zhang Y, Liu Y, Liu S, Zhang X (2012) Dynamics of stand biomass and volume of the tree layer in forests with different restoration approaches based on tree-ring analysis. *Chin J Plant Ecol* 36:117–125 (in Chinese with English abstract)
- Zhang C, Zhao X, von Gadow K (2015) Maximum density patterns in two natural forests: an analysis based on large observational field studies in China. *For Ecol Manag* 346:98–105. doi:[10.1016/j.foreco.2015.03.001](https://doi.org/10.1016/j.foreco.2015.03.001)
- Zhao M, Xiang W, Peng C, Tian D (2009) Simulating age-related changes in carbon storage and allocation in a Chinese fir plantation growing in southern China using the 3-PG model. *For Ecol Manag* 257: 1520–1531. doi:[10.1016/j.foreco.2008.12.025](https://doi.org/10.1016/j.foreco.2008.12.025)
- Zianis D, Mencuccini M (2005) Aboveground net primary productivity of a beech (*Fagus moesiaca*) forest: a case study of Naousa forest, northern Greece. *Tree Physiol* 25:713–722. doi:[10.1093/treephys/25.6.713](https://doi.org/10.1093/treephys/25.6.713)